Indian Journal of Pure & Applied Physics
Vol. 58, April 2020, pp. 218-222

Measurement of $^{92}\mathrm{Mo}(n,\alpha)^{89}\mathrm{Zr}$ and $^{97}\mathrm{Mo}(n,p)^{97}\mathrm{Nb}$ reactions at the neutron energy 13.52 MeV with covariance analysis

A M Sunitha[a], B Rudraswamy[a], S V Suryanarayana[b], Kamsali Nagaraja[a], Meghna Karkera[c], Imran Pasha[a], H B Sachhidananda[d], Y S Sheela[c] & Manjunatha Prasad[c]

[a]Department of Physics, Bangalore University, Bengaluru 560 056, India
[b]Nuclear Physics Division, Bhabha Atomic Research Center, Mumbai 400 085, India
[c]Department of Data Science, Manipal Academy of Higher Education, Manipal 576 104, India
[d]Visvesvaraya Technological University, Belgaum 590 018, India

Received 17 February 2020

The cross sections have been estimated for the Nuclear reactions $^{92}\mathrm{Mo}(n,\alpha)^{89}\mathrm{Zr}$ and $^{97}\mathrm{Mo}(n,p)^{97}\mathrm{Nb}$ produced in Purnima neutron generator at neutron energy of 13.52±0.0045 MeV using activation analysis and off-line γ -ray spectrometric techniques. $^{27}\mathrm{Al}(n,\alpha)^{24}\mathrm{Na}$ has been used as a monitor reaction. The covariance analysis for these cross sections has been carried out by taking into consideration of partial uncertainties of different attributes and correlations between the attributes. The cross section values of the present study have been compared with EXFOR, ENDF data of various libraries and theoretical data of TALYS-1.8 code.

Keywords: $^{92}\mathrm{Mo}(n,\alpha)^{89}\mathrm{Zr}$,$^{97}\mathrm{Mo}(n,p)^{97}\mathrm{Nb}$, Reaction cross section, Activation analysis, Covariance, TALYS-1.8.

1 Introduction

Nuclear reaction cross-section is one of the most important measurable quantities in the field of nuclear and particle physics. Neutron cross section plays an important role in the nuclear transmutation, nuclear reactions, radiation damage and other phenomena[1]. The activation foil such as Molybdenum (Mo) used in the present reactions forms an important constituent in the first wall of fusion reactor and its cross section value is used in the construction of different types of nuclear reactors[2-5]. Accurate neutron induced reaction cross section data of Mo isotopes are important for reaction mechanism, nuclear structure, neutron dosimetry, radiation damage to materials, activation analysis and shielding. It finds applications in biomedical, cancer therapy, production of radio-isotopes. As a consequence, it has a wide potential for use in neutronic applications such as an accelerator-driven system and controlled nuclear fusion device.

The cross sections have been estimated for the Nuclear reactions $^{92}\mathrm{Mo}(n,\alpha)^{89}\mathrm{Zr}$ and $^{97}\mathrm{Mo}(n,p)^{97}\mathrm{Nb}$ produced in Purnima neutron generator at neutron energy of 13.52±0.0045 MeV using activation analysis and off-line γ -ray spectrometric techniques. $^{27}\mathrm{Al}(n,\alpha)^{24}\mathrm{Na}$ has been used as a monitor reaction. The covariance analysis for these cross sections has been carried out by taking into consideration of partial uncertainties of different attributes and correlations between the attributes. The cross section values of the present study have been compared with EXFOR, ENDF data of various libraries and theoretical data of TALYS-1.8 code.

2 Experimental Details

The experiment has been carried out with neutron generator which works on the principle of Cockcroft-Walton voltage multiplier accelerator of PURNIMA at BARC, Mumbai. In the present measurement, D^+ ion has been accelerated to 99.71 keV to impinge on Titanium–Tritium (Ti-T) target. The resulting mono-energetic neutron of energy 13.52±0.0045 MeV from reaction $^{3}\mathrm{H}(d,n)^{4}\mathrm{He}$ (Q=17.59 MeV) has been used as a projectile to bombard activation foils such as Molybdenum (Mo) and aluminium (Al) to obtain the given reactions. The γ-ray counting of the resulting reaction product has been carried out using lead shielded precalibrated185-cc Baltic HPGe detector having 30% relative efficiency coupled to PC-based 4k multi channel analyser.

In our experimental set up, the area of target covers an angle of ((1cm)/((2 * pi * 1.5 cm) * (180°))) ~ 19.1°. The Mo sample has a purity of 99.9% and has a rectangle-shaped with0.0049mm thick. Each of the

---

*Corresponding author
(E-mail: kamsalinagaraj@gmail.com and brudraswamy@gmail.com)

samples ^{92}Mo, ^{97}Mo and ^{27}Al have weights 0.1988g, 0.1988g and 0.0297g, respectively. They have been wrapped with 0.0063 mm thick Al foil to shield the radioactive contamination from one another during the neutron irradiation. The foil has been mounted at zero degree angle relative to the beam direction. The Mo and Al foils have been irradiated together for 1.5 h with neutron beam coming from the ^{3}H(d,n)^{4}He reaction. After the irradiation, the foils have been taken out and cooled for 0.2217 to 99.60 h.

The counting dead time has always kept less than 5% by placing the irradiated Mo sample at a distance of 1 cm from the end cap of the detector. The energy and efficiency calibration of the detector system have been performed by using standard ^{152}Eu source, keeping the same geometry to reduce coincidence summing effect. The resolution of the detector system has FWHM of 1.8 keV at 1332.5 keV of ^{60}Co. The data acquisition has been done using a CAMAC based LAMPS (Linux Advance Multi Parameter System) software. The γ-ray activity of ^{27}Al produced from the ^{27}Al(n,α)^{24}Na monitor reaction has been used to measure the neutron flux.

3 Results and Discussion

3.1 Determination of efficiency calibration with covariance analysis

Standard point ^{152}Eu source has been used for characteristic γ-ray energy efficiency $\varepsilon(E_\gamma)$ calibration of the HPGe detector system. The efficiency of HPGe detector system has been estimated by the following relation:

$$\varepsilon(E\gamma) = \frac{CK_c}{I_\gamma A_0\, e^{\left(\frac{-0.693\,t}{T_{\frac{1}{2}}}\right)}} \quad \ldots (1)$$

where $\varepsilon(E_\gamma)$ is the efficiency of the detector, C is the detected γ-ray counts under the photo-peak per second, K_c is the correction factor for the coincidence summing effect, I_γ is the γ-ray abundance, A_o (6659.21 ± 81.60 Bq as on 1 October 1999) is the calibration source activity at the time of packing, $T_{1/2}$(13.517 ± 0.014 y) is the half-life of radioactive nuclide and t (18.53 y) is the time elapsed between calibration at the time of packing and at the time of the experiment. The decay data for half-life and γ-ray abundance for the efficiency calibration has been taken from NuDat[6]. The correction factor for coincidence summing given in Eq. (1) to obtained efficiency $\varepsilon(E\gamma)$ (using the Monte Carlo simulation code EFFTRAN[7]) at each of the specified γ-ray energy of ^{152}Eu source and the same are presented in column 5 of Table 1.

C, I_γ , A_o and $T_{1/2}$ are the four attributes observed with uncertainty, which contributes to the uncertainty in efficiency. The partial uncertainties due to each of the attributes mentioned above and their correlations for constructing the covariance matrix V_ϵ have been obtained by following the methodology[8, 9].
We choose the linear parametric function,

$$Z = \ln(\varepsilon_i) = \sum_{k=1}^{m} p_k\ (\ln[E_i\,])^{k-1}\ \ 1 \le i \le 8, 1 \le k \le m \quad \ldots (2)$$

We further obtained the linear parametric function $\ln\varepsilon_i = -3.8824 - 0.8802(\ln E) + 0.05478(\ln E)^2$. The least square condition states that the best estimate for parameter vector p in the model is the one which minimizes the Chi-square statistics. In the present case we obtained:

$$\frac{\chi^2}{n-m} = \frac{\chi^2}{8-3} = 1.011 \quad \ldots (3)$$

where n is the numbers of γ-ray energies (in the present case n=8) and m is the number of parameters. The methodology is defined in early study[8] and we have followed the methods stated in previous studies[10-12] to estimate efficiency at the characteristic γ-ray energies of the reaction products corresponding to the sample nuclide ^{89}Zr, ^{97}Nb and the monitor nuclide ^{24}Na with its covariance error matrix. The numerical results of the same are presented in Table 2.

Table 1 — HPGe detector efficiency calibration based on standard ^{152}Eu source

Eγ (keV)	Iγ (%)	C	K_c	$\varepsilon(E_\gamma)$
244.697	7.55 ± 0.04	11566.09 ± 226.6	1.35	0.0795
344.3	26.59 ± 0.2	33616.98 ± 339.41	1.151	0.0559
411.1	2.237 ± 0.13	1967.05 ± 76.55	1.405	0.0475
778.9	12.93 ± 0.08	7160.83 ± 121.95	1.23	0.0262
867.4	4.23 ± 0.03	1831.09 ± 84.98	1.424	0.0237
1085.84	10.11 ± 0.05	5291.69 ± 144.57	0.901	0.0181
1112.08	13.67 ± 0.08	6123.09 ± 135.33	1.088	0.0187
1408.013	20.87 ± 0.09	7493.86 ± 111.04	1.121	0.0155

Table 2 — Interpolated detector efficiencies

Radio nuclide	γ-ray energy (keV)	Efficiency	Correlation matrix		
^{92}Mo	910.005	0.0224 ± 0.00037	1		
^{97}Mo	657.94	0.0301 ± 0.00056	0.6402	1	
^{27}Al	1368.626	0.0157 ± 0.00028	0.3956	0.9546	1

3.2 Estimation of cross sections ^{92}Mo(n,α)^{89}Zr and ^{97}Mo(n,p)^{97}Nb reaction with covariance analysis

The cross section of ^{92}Mo(n,α)^{89}Zr and ^{97}Mo (n,p)^{97}Nb reaction at the effective neutron energy of13.52±0.0045 MeV has been estimated by using the following equation:

$$\sigma_s(E_n) = \left[\frac{\sigma_m(En)\ C_s\,\lambda_s\ Wt_m\ abn_m\ Av_s\ I\gamma_m\ \epsilon\gamma_m\left(1-e^{-\lambda_m t_{irrm}}\right)\left(e^{-\lambda_m t_{coolm}}\right)\left(1-e^{-\lambda_m t_{cm}}\right)}{C_m\ \lambda_m\ Wt_s\ abn_s\ Av_m\ I\gamma_s\ \epsilon\gamma_s\left(1-e^{-\lambda_s t_{irrs}}\right)\left(e^{-\lambda_s t_{cools}}\right)\left(1-e^{-\lambda_s t_{cs}}\right)}\right]\pi_k\left(\frac{Ck_m}{Ck_s}\right) \quad \ldots (3)$$

Where s and m subscripts represent the sample and monitor,$\sigma_s(E_n)$ and $\sigma_m(E_n)$ are cross sections of ^{92}Mo(n,α)^{89}Zr ,^{97}Mo(n,p)^{97}Nband ^{27}Al(n,α)^{24}Na respectively.$C_s \lambda_s$,Wt_s, abn_s, Av_s, $I\gamma_s$ and $\varepsilon(E_\gamma)_s$ are the γ-ray peak counts, decay constant, weight, isotopic abundance, average atomic mass, γ- ray abundance and efficiency of the sample reactions respectively. C_m, λ_m, Wt_m abn_m, Av_m, $I\gamma_m$ and $\varepsilon(E_\gamma)_m$ are the γ-ray peak counts, decay constant, weight, isotopic abundance, average atomic mass, γ-ray abundance and efficiency of the monitor reaction respectively. t_{irru}, t_{coolu}, t_{counu} , t_{irrm}, t_{coolm} and t_{counm} are irradiation, cooling and counting time for the sample and monitor respectively, $(Ck)_s$ and $(Ck)_m$ are the correction factors of the kth attributes which includes the dead time correction factor of the HPGe detector, $(\frac{\text{Clock time}}{\text{Live time}})$ and γ-ray self attenuation correction factor g_{attn} .of sample and monitor, respectively. The γ-ray self-attenuation factor (g_{attn}.) for the activation foils were obtained by using the relation, $g_{attn} = \frac{1-e^{-\mu l}}{\mu l}$ where μ is the mass attenuation co-efficient and l is the thickness of the sample obtained using the XMuDat Ver. 1.01 [13,14].

For the purpose of covariance analysis, among all the attributes appearing in Eq (3), the uncertainty in the attributes observed with error σ_m, C_s, λ_s, Wt_s, Av_s, $I\gamma_s$, $\varepsilon(E\gamma)_s$, abn_s, $(g_{attn})_s$, C_m, λ_m, Wt_m, Av_m, $I\gamma_m$, $(g_{attn})_m$, and $\varepsilon(E\gamma)_m$ are propagated in order to obtain uncertainty in the sample reaction cross section. Other attributes namely, t_{irr}, t_{cool} and t_{count} have been observed without error and are treated as constants. The decay data, such as half-life, γ-ray abundances, isotopic abundances and average atomic mass with its associated uncertainties are presented in Table 3 and are retrieved from NUDat 2.7 database[15]. The monitor ^{27}Al(n,α)^{24}Na reaction cross section at neutron energy 13.52 MeV was obtained by using linear interpolation method from the evaluated data available in the IRDF -2002G.

Table 3 — Basic data required for estimation of $\sigma_u(E_n)$

Nuclear reaction	γ-ray energy (keV)	Half-life	Isotopic abundance (%)	γ-ray abundance (%)
^{92}Mo(n,α)^{89}Zr	909.15 ± 0.15	78.41 ± 0.12h	14.53±0.3	99.04
^{97}Mo(n,p)^{97}Nb	657.9 ± 0.09	72.1 ± 0.7m	9.6±0.14	98.23
^{27}Al(n,α)^{24}Na	1368.63 ± 0.005	14.997 ± 0.012h	100	99.99 ± 0.0015

The covariance matrix $V_{\sigma U}$ [11] corresponding to the experimentally measured reaction cross section data is given by

$$(V_{\sigma U})_{ij} = \sum_{kl}(e_k)_i(S_{kl})_{ij}\,(e_l)_j,\ 1 \le i,j \le 2, 1 \le k,l \le 16 \quad \ldots (4)$$

where, $(e_k)_i = \frac{\partial\sigma_{Ui}}{\partial(x_k)_i}\Delta(x_k)_i$ is the partial uncertainty in σ_{Ui} due to ith observation of kth attribute and $(e_l)_j = \frac{\partial\sigma_{Uj}}{\partial(x_l)_j}\Delta(x_l)_j$ is the partial uncertainty in σ_{Uj} due to jth observation of lth attribute,

σ_{Ui} and σ_{Uj} represent vectors of two reaction (^{92}Mo(n,α)^{89}Zr and ^{97}Mo(n,p)^{97}Nb) cross section, $\Delta(x_k)_i$ and $\Delta(x_l)_j$ are the uncertainties associated with the ith and jth observation of kth and lth attributes and $(S_{kl})_{ij}$ is represent the micro correlation (correlation between the observations(ij) and attributes (kl)). The partial uncertainties from different attributes present in the measured reactions of ^{92}Mo(n,α)^{89}Zr and ^{97}Mo(n,p)^{97}Nb cross section with respect to ^{27}Al(n,α)^{24}Na monitor reaction are listed in Table 4. The correlations obtained between two observations are listed in the column 4 of Table 4. For the detailed derivation of Eq. (4) with necessary description, the readers can refer to the reference by Santhi Sheela *et al.* [16]. Table 5 presents the results of the measured ^{92}Mo(n,α)^{89}Zr and ^{97}Mo(n,p)^{97}Nb reaction cross section at the neutron energy of 13.52 MeV.

4 Discussion

In our present study, the ^{92}Mo(n,α)^{89}Zr and ^{97}Mo(n,p)^{97}Nb reaction cross section have been measured relative to the cross section of ^{27}Al(n,α)^{24}Na at the neutron energy of 13.52±0.0045 MeV by the activation and off-line γ-ray spectrometric techniques.

The computer code TALYS-1.8 has been used to generate ^{92}Mo(n,α)^{89}Zr and ^{97}Mo(n,p)^{97}Nb reaction

Table 4 — Partial uncertainties and correlations from the different attributes of measured reactions relative to monitor reaction

Attributes	^{92}Mo(n,α)^{89}Zr	^{97}Mo(n,p)^{97}Nb	Correlation
Monitor reaction cross section σ_m	1.9954E-04	1.8271E-04	Correlated
γ-ray peak counts C_m	1.0794E-03	9.8841E-04	Fully Correlated
Decay constant λ_m	4.81499E-06	4.40897E-06	Fully correlated
Weight of monitor Wt_m	4.87702E-05	4.4658E-05	Fully correlated
Monit Average atomic mass Av_m	4.6492E-11	4.2571E-11	Fully correlated
γ-ray abundance I_m	3.7635E-07	3.4461E-07	Fully correlated
Efficiency of detector $\varepsilon(E_\gamma)_m$	7.8805E-04	7.216E-04	Fully correlated
γ-attenuation coefficient $(g_{attn})_m$	6.54895E-04	5.9967E-04	Fully correlated
γ-ray peak counts C_s	9.6925E-03	3.2352E-03	Uncorrelated
Decay constant λ_s	4.30902E-06	4.1797E-05	Uncorrelated
Weight of sample Wt_s	7.2861E-06	6.6717E-06	Fully correlated
Isotopic abundance abn_s	5.17997E-04	3.3502E-04	Uncorrelated
Sample average atomic mass Av_s	4.6406E-11	4.2671E-11	Uncorrelated
Efficiency of detector$\varepsilon(E_\gamma)_s$	4.2829E-04	4.4073E-04	Uncorrelated
γ-attenuation coefficient$(g_{attn})_s$	7.7042E-04	8.4891E-04	Correlated

Table 5 — The measured reaction cross-sections relative to the monitor ^{27}Al(n,α)^{24}Na reaction cross-section with its correlation matrix

Reaction	Cross-section (barns)	Correlation Matrix	
^{92}Mo(n,α)^{89}Zr	0.0257 ± 0.01	1	
^{97}Mo(n,p)^{97}Nb	0.0179 ± 0.002	0.2268	1

cross section data from threshold to 20 MeV, compared with the present data and is depicted as shown in Fig.1 and Fig. 2. We present our experimental data of ^{92}Mo(n,α)^{89}Zr reaction at neutron energy of 13.52±0.0045 MeV, the literature data [17-24] from EXFOR[25], evaluated data from ENDF/B-V111.0[26], JEFF-3.3[27], JENDL-4.0[28], ROSFOND-2010[29], CENDEL-3.1[30] libraries and theoretical model based code TALYS -1.8[31] in the default parameter mode.

It is observed from Fig. 1 that the ^{92}Mo(n,α)^{89}Zr reaction cross section of our experimental data at neutron energy of 13.52±0.0045 MeV is in good agreement with the all evaluated data libraries ENDF/B-V111.0[26], JEFF-3.3[27], JENDL-4.0[28], ROSFOND-2010[29], CENDL-3.1[30], literature data [17-24] from EXFOR[25] but shows large variation among the literature data of Y. Kanda (1972) higher than the theoretically estimated values from TALYS-1.8[31] and evaluated data libraries.

It is observed from Fig.1 that the ^{92}Mo(n,α)^{89}Zr reaction cross section of our experimental data at neutron energy of 13.52±0.0045 MeV is in good agreement with the all evaluated data libraries ENDF/B-V111.0[26], JEFF-3.3[27], JENDL-4.0[28], ROSFOND-2010[29], CENDL-3.1[30], literature data [17-24] from EXFOR[25]

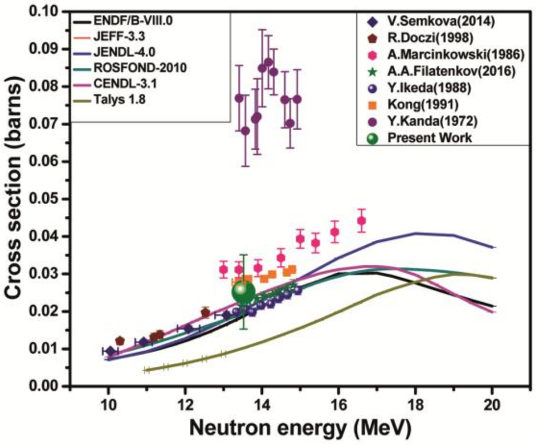

Fig. 1 — Comparison of ^{92}Mo(n,α)^{89}Zr reaction cross section from the present work with the evaluated data from different libraries and theoretical values from TALYS-1.8

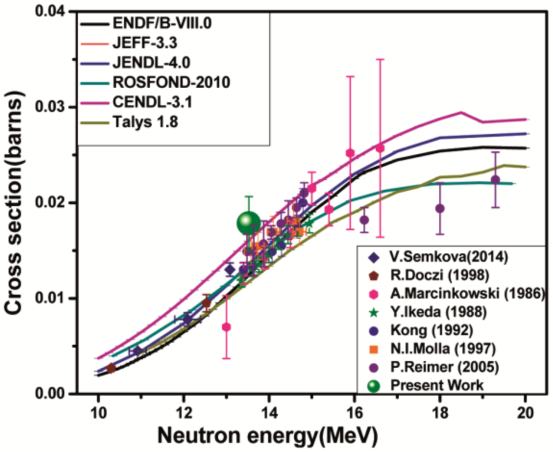

Fig. 2 — Comparison of ^{97}Mo(n,p)^{97}Nb reaction cross section from the present work with the evaluated data from different libraries and theoretical values from TALYS-1.8

For, the experimentally measured ^{97}Mo(n,p)^{97}Nb reaction cross section at the neutron energy 13.52±0.0045 MeV, the evaluated data files ENDF/B-V111[26], JEFF-3.3[27], JENDL-4.0[28], ROSFOND-2010[29], CENDL-3.1[30] data libraries, literature data [17-24] from EXFOR[25], as well as the theoretical values from TALYS-1.8[31] within the neutron energies 10-20 MeV are shown in Fig. 2. It can seen from Fig. 2 that the ^{97}Mo(n,p)^{97}Nb reaction cross section of the present work at the effective neutron energy of 13.52±0.0045 MeV is found to be good agreement with the estimated values from TALYS-1.8, evaluated data files and literature data[17-24] from EXFOR[25].

5 Conclusions

The cross sections of ^{92}Mo(n,α)^{89}Zr and ^{97}Mo(n,p)^{97}Nb reactions of the present work have been compared with other data and found to be in good agreement with the literature data.

Acknowledgement

The author would like to thank the staff of Purnima neutron generator division of BARC, Mumbai for providing experimental facilities.

References

1 Zhao W, Lu H, Yu W & Yuan X, *Compilation of measurement and evaluations of nuclear activation cross section for nuclear data applications*, INDC (CPR) (1989) 16.

2 Amemiya S, Ishibashi K & Katoh T, *J Nucl Sci Technol*, 19 (1982) 781.

3 Fessler A, Plompen A J M, Smith D L, Meadows J W & Ikeda Y, *Nucl Sci Eng*, 134 (2000) 200.

4 Garlea I, Miron-Garlea C, Rosh H N, Fodor G & Raduch V, *J Revue Roumaine de Phys*, 37 (1992) 19.

5 Amemiya S, Ishibashi K & Katoh T, *J Nucl Sci Technol*, 19 (1982) 781.

6 Sonzogni A, NuDat 2.6 (as of April 17, 2017), National Nuclear Data Centre, Brookhaven National Laboratory, http://www.nndc.bnl.gov/(2017).

7 Vidmar T, *Nucl Instrum Meth Phys Res*, 550 (2005) 603.

8 Geraldo L P & Smith D L, *Nucl Instrum Meth Phys Res A*, 290 (1990) 499.

9 Pasha I, Rudraswamy B, Radha E & Sathiamoorthy V, *Radiat Prot Environ*, 41 (2018) 110.

10 Shivashankar B S, Ganesan S, Naik H, Suryanarayana S V, Nair N S & Prasad K M, *Nucl Sci Eng*, 179 (2015) 423.

11 Yerraguntla S S, Naik H, Karantha M P, Ganesan S, Suryanarayana S V & Badwar S J, *Radioanal Nucl Chem*, 314 (2017) 457.

12 Ganesan S, *Nucl Data Sheets*, 123 (2015) 21.

13 Millsap D W, *Appl Radiat Isotopes*, 97 (2015) 433.

14 Nowotny R XMuDat: Photon attenuation data on PC, IAEA Report IAEA-NDS, https://www- nds.iaea.org/publications/iaea-nds/ iaea-nds-0195.htm, 195 (1998).

15 NuDat 2.7 National Nuclear Data Center, Brookhaven National Laboratory. http://www.nndc.bnl.gov/nudat 2(2016)

16 Santhi S, Naik H, Prasad K M, Ganesan S, Nair N S & Suryanarayana S V, Covariance analysis of efficiency calibration of HPGe detector. Internal Report, No. MU/ STATISTICS/DAE-BRNS/2017/1,https://doi.org/10.13140/rg.2.2.32025.21605, 19 February-2017

17 Semkova V & Nolte R, *EPJ Web*, 66 (2014) 03077.

18 Marcinkowski A, Stankiewicz K, Garuska U & Herman M, Cross sections of fast neutron induced reactions on molybdenum isotopeshttps://link.springer.com/journal/218(1986) 91.

19 Filatenkov A A, Neutron activation cross sections measured at KRI in neutron energy region 13.4-14.9 MeV, INDC (CCP) (2016) 0406.

20 Ikeda Y, Konno C, Oishi K, Nakamura T, Miyade H, Kawade K, Yamamoto H & Katoh T, Activation cross section measurement for fusion reactor structural materials at neutron energy from 13.3 to 15.0 MeV using FNS facility, Report JAERI, 1312 (1988).

21 Kanda Y, *Nucl Phys A*, 177 (1972) 195.

22 Kong X, Wang Y, Yuan J & Yang J, *J Lanzhou Univ*, 0455 (1996) 2059.

23 Molla N I, Miah R U, Sasunia S, Houssain S M & Rahman M, *TRIEST C*, 97 (1997) 517.

24 Reimer P, Avrigeanu V, Chuvaev S V, Filatenkov A A, Glodariu T, Koning A, Plompen A J M, Qaim S M Smith D L & Weigmann H, *Phys Rev C*, 71 (2005) 044617.

25 IAEA-EXFOR Database available at http://www-nds.iaea.org/exfor.

26 Chadwick M, Herman M, Oblozinsky P, Dunn M E, Danon Y, Kahler A, Smith D L, Pritychenko B, Arbanas G, Arcilla R,Brewer R, Brown D A, Capote R, Carlson A D, Cho Y S, Derrien H, Guber K, Hale G M, Hoblit S, Holloway S, Johnson T D, Kawano T, Kiedrowski B C, Kim H, Kunieda S, Larson N M, Leal L, Lestone J P, Little R C, McCutchan E A, MacFarlane R E, MacInnes M, Mattoon C M, McKnight R D, Mughabghab S F, Nobre G P A, Palmiotti G, Palumbo A, Pigni M T, Pronyaev V G, Sayer R O, Sonzogni A A, Summers N C, Talou P, Thompson I J, Trkov A, Vogt R L, van der Marck S C, Wallner A, White M C, Wiarda D, Young P G, *Nucl Data Sheets*, 112 (2011) 2996.

27 An International collaboration of NEA data bank participating countries The Joint Evaluated Fission and Fusion File (JEFF). http://www.oecd-nea.org(2017).

28 Shibata K, Iwamoto O, Nakagawa T, Iwamoto N, Ichihara A, Kunieda S, Chiba S, Furutaka K, Otuka N, Ohasawa T, Murata T, Matsunobu H, Zukeran A, Kamada S & Katakura J, *J Nucl Sci Technol*, 48 (2011) 30.

29 Zabrodskaya S V, Ignatyuk A V & Koscheev V N, *Nucl Constants*, 1 (2007) 2.

30 Ge Z G, Zhao Z X, Xia H H, Zhuang Y X, Liu T J, Zhang J S & Wu H C, *J Korean Phys Soc*, 59 (2011) 1052.

31 Koning A J, Hilaire S & Goriely S, TALYS-1.8, A Nuclear Reaction Program (NRG-1755 ZG Petten, The Netherlands). http://www.talys.eu/download-talys/ (2015).